The Asparagine-Stabilized β-Turn of Apamin: Contribution to Structural Stability from Dynamics Simulation and Amide Hydrogen Exchange Analysis†

Christopher E. Dempsey,* Richard B. Sessions, Nicole V. Lamble, and Stephen J. Campbell

Biochemistry Department and Centre for Molecular Recognition, School of Medical Sciences, University of Bristol, Bristol BS8 1TD, United Kingdom

Received August 29, 2000; Revised Manuscript Received October 31, 2000

ABSTRACT: Molecular dynamics simulations of bee venom apamin, and an analogue having an Asn to Ala substitution at residue 2 (apamin-N2A), were analyzed to explore the contribution of hydrogen bonds involving Asn2 to local (β-turn residues N2, C3, K4, A5) and global stability. The wild-type peptide retained a stable conformation during 2.4 ns of simulation at 67 °C, with high β-turn stability characterized by backbone−side chain hydrogen bonds involving β-turn residues K4 and A5, with the N2 side chain amide carbonyl. The loss of stabilizing interactions involving the N2 side chain resulted in the loss of the β-turn conformation in the apamin N2A simulations (27 or 67 °C). This loss of β-turn stability propagates throughout the peptide structure, with destabilization of the C-terminal helix connected to the N-terminal region by two disulfide bonds. Backbone stability in a synthetic peptide analogue (apamin-N2A) was characterized by NMR and amide hydrogen exchange measurements. Consistent with the simulations, loss of hydrogen bonds involving the N2 side chain resulted in destabilization of both the N-terminal β-turn and the C-terminal helix. Amide exchange protection factors in the C-terminal helix were reduced by 9−11-fold in apamin N2A as compared with apamin, corresponding to free energy ($\delta\Delta G_{uf}$) of around 1.5 kcal M^{-1} at 20 °C. This is equivalent to the contribution of hydrogen bond interactions involving the N2 side chain to the stability of the β-turn. Together with additional measures of exchange protection factors, the three main contributions to backbone stability in apamin that account for virtually the full thermodynamic stability of the peptide have been quantitated.

Position-specific propensities for amino acid residues in β-turns have been identified from the frequencies of amino acid occurrences in β-turns of proteins in the structural database (*1*). Unlike the case of amino acid α-helical (*2, 3*) and β-sheet propensities (*4*), where contributions to secondary structural stability in terms of amino acid-specific free energies have been quantitated, the thermodynamics of β-turn amino acid propensities are not well characterized. This results from the low intrinsic stability of the β-turn in isolation, the lack of a convenient spectroscopic signal (analogous to the CD signature of the α-helix) that would allow simple quantitation of β-turn content in suitable host-guest peptides, the tendency for peptides in β-conformations to aggregate in aqueous solution (*5, 6*), and the contribution of nonlocal interactions to β-turn stabilities in proteins that limits a systematic mutational approach to the thermodynamics of β-turn amino acid propensities (e.g., ref *7*).

Several strong positional preferences in β-turns have been identified, including the preference for Pro at position i + 1 of type I and II turns, Gly at specific positions in several types of turn, and Asp or Asn at position i of a type I β-turn (*1, 8*). Bee venom apamin (*9*) contains a β-turn (Asn2−Cys3−Lys4−Ala5) with Asn in the i position (*10*), which is characteristic of an Asn-stabilized β-turn. The N-terminal sequence of apamin containing the β-turn is connected by two disulfide bonds to a C-terminal α-helix (Figures 1 and 2). As a result, the peptide has a well-defined structure (refs *10* and *11*; Figure 2) with high conformational stability (*12*−*14*), typical of this class of channel binding peptide toxins (*15*). In the classical Asn-stabilized β-turn motif [see recent

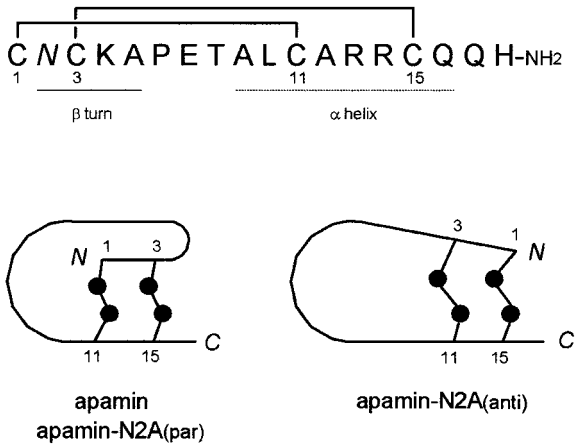

FIGURE 1: Amino acid sequence and disulfide pairing of apamin. Residue 2 (italicized) is alanine in apamin-N2A. The disulfide pairings of apamin-N2A(par) and apamin-N2A(anti) are also illustrated. Note that apamin analogues having the (par)allel and (anti)parallel disulfide pairings are designated "globule" and "ribbon", respectively, in the notation of Pegoraro et al. (*32*).

† This research was supported by a grant from the Joint Research and Equipment Initiative (JREI) of the Biotechnology and Biological Sciences Research Council.

* To whom correspondence should be addressed. Telephone: (0)-117 928 7427. Fax: (0)117 928 8274. E-mail: c.dempsey@bris.ac.uk.

10.1021/bi002044q CCC: $19.00
Published on Web 12/01/2000

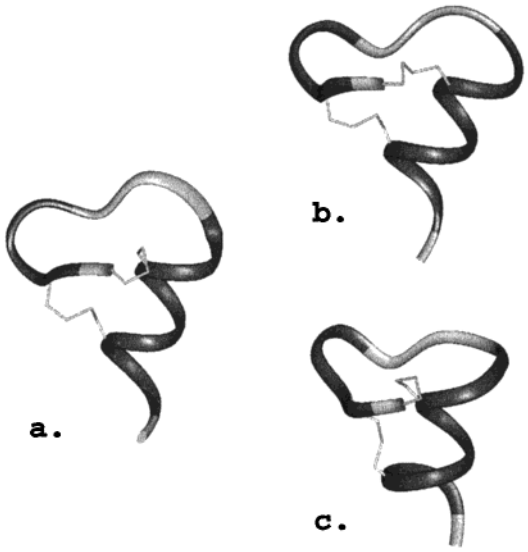

FIGURE 2: Starting (a) and final (b) structure of apamin (2.4 ns) and (c) apamin-N2A(par) (2 ns) after molecular dynamics simulation at 67 °C. The starting structure for the apamin-N2A(par) simulation was the apamin coordinates with Asn2 replaced with Ala, so that the ribbon representing the apamin and apamin-N2A(par) starting structures (a) are equivalent.

classification of Wan and Milner-White (*16*)], a side chain to main chain hydrogen bond involving Asn i side chain amide and the backbone NH of residue i + 2 supplements the β-turn hydrogen bond involving the backbone amide NH and amide carbonyl of residues i + 3 and i, respectively. These hydrogen bonds (i.e., Lys4 NH with Asn2 side chain amide carbonyl, and Ala5 NH with Asn2 backbone carbonyl in apamin) are proposed to account for the slow hydrogen−deuterium exchange of Ala5 and Lys4 backbone amide hydrogens (*11*).

We have run molecular dynamics simulations to characterize hydrogen bonding in the Asn-stabilized β-turn motif in apamin for comparison with amide hydrogen exchange measurements of hydrogen bond stabilities. As described here, replacing Asn2 with alanine in the starting structure results in loss of conformational stability throughout the polypeptide, including the C-terminal α-helix, during simulations in water. This is consistent with observations from amide exchange analysis that the conformational stabilities of the N-terminal β-turn and C-terminal helix are linked; i.e., Ala5 NH and amides in the stable region of helix (Ala12−Cys15 NHs) share similar H/D exchange properties (*14*). This thermodynamic linkage should allow quantitation of the contribution of Asn2 side chain interactions to stabilization of the N-terminal β-turn through their effects on stability of the C-terminal helix. We have made the alanine-substituted apamin analogue (apamin-N2A)[1] and describe here the effects of the mutation on the folding, conformation, and stability of apamin.

MATERIALS AND METHODS

Materials. Apamin was purified from bee venom by HPLC. Apamin-N2A, and an additional sample of wild-type apamin, were synthesized by Dr. Graham Bloomberg of the Bristol Molecular Recognition Centre, using Fmoc solid-phase chemistry. The crude peptides were purified by HPLC on a Vydac C4 reverse-phase column using a gradient of acetonitrile (5−18%) in water containing 0.1% TFA. The purity and integrity of the peptides were confirmed by mass spectrometry. Air oxidation of the purified synthetic peptides was achieved by dissolving in 10 mM sodium phosphate, pH 7.0, at a concentration of 1 mg mL^{-1} and leaving unstirred at room temperature until oxidation was complete. Oxidative formation of disulfide bonds was monitored by reverse phase HPLC. The oxidized peptides were purified by HPLC, and their purity and integrity were confirmed by mass spectrometry and by assignment of the high-resolution NMR spectra in water.

NMR Spectroscopy. One- and two-dimensional NMR spectra were obtained on the 500 MHz JEOL NMR spectrometer of the Bristol Centre for Molecular Recognition using standard methods (*17*).

Amide Hydrogen−Deuterium Exchange Rates. Amide exchange rates were measured by dissolving samples of lyophilized peptide in buffer made in D_2O and collecting spectra throughout an exchange time-course at 20 °C. The buffer was 25 mM glycine and 25 mM sodium acetate to cover the pH* range 2.0−4.5, where pH* is the pH measured using a hydrogen electrode. Random coil exchange rates were calculated using eq 1, where k_H, k_{OH}, and k_W are the acid-catalyzed, base-catalyzed, and pH-independent exchange rate constants for poly-D, L-alanine (PDLA) (*18*). The value of pH used in eq 1 was the measured pH* plus 0.4 to correct for the deuterium isotope effect on the hydrogen electrode, plus an additional value of 0.3 to correct for the global charge effect that results in an enhancement of base-catalyzed exchange and suppression of acid-catalyzed exchange due to the high fixed charge of apamin (+5 at low pH). The latter value was obtained using the data of Kim and Baldwin (*19*), by estimating the effect on the acid- and base-catalyzed exchange rate constants of amide exchange from poly-D, L-lysine (PDLK) at an ionic strength corresponding to 50 mM buffer ions as compared with 400 mM buffer ions and scaling for the reduced charge density of apamin as compared with PDLK. Random coil exchange rates from eq 1 were additionally corrected for sequence-dependent contributions tabulated by Bai et al. (*18*). Exchange protection factors are the residue-specific corrected value of k_{PDLA} divided by the experimental exchange rate constant.

$$k_{PDLA} = k_H 10^{-pH} + k_{OH} 10^{(pH - 15.05)} + k_W \qquad (1)$$

Molecular Dynamics Simulations. MD simulations were run at constant volume under periodic boundary conditions using protocols similar to those previously described (*20*, *21*). The starting structure for MD simulations was obtained from the coordinates of the NMR structure of Pease and Wemmer (*11*). Coordinate set 1 of the family of six coordinate sets that satisfy the NMR structural constraints (*11*) was chosen by random selection, for use in the simulations. The peptide was placed in the center of a 35-Å cubic box of water and energy minimized for 3000 steps of conjugate gradients. Dynamics simulations were started at the required

[1] Abbreviations: apamin-N2A(par), N2A substitution analogue of apamin having wild-type disulphide pairings; apamin-N2A(anti), N2A substitution analogue of apamin having non-wild-type (endothelin-like) disulphide pairings (i.e., Cys1 with Cys15, and Cys3 with Cys 11); HPLC, high-performance liquid chromatography; NMR, nuclear magnetic resonance.

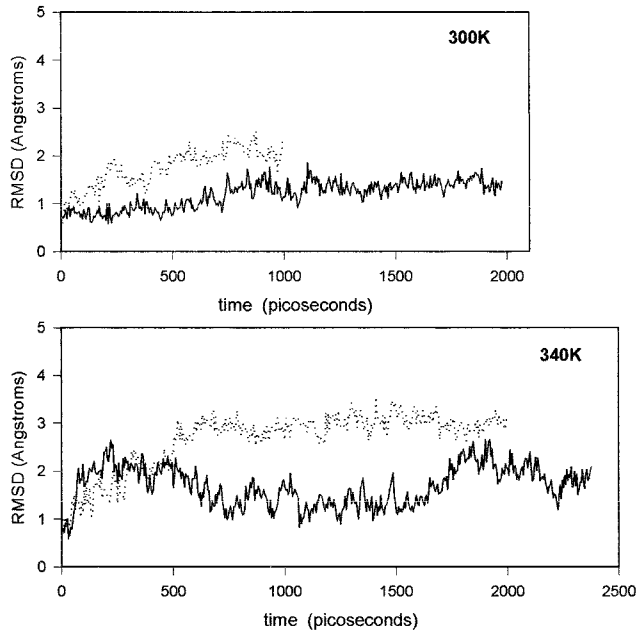

FIGURE 3: RMSD of backbone atoms of apamin (bold traces) and apamin-N2A(par) (light traces) during molecular dynamics simulation in water at 27 °C (top) and 67 °C (bottom).

temperature (300 or 340 K) by assigning random velocities of appropriate magnitude to all atoms. Structures were saved every 1 ps for subsequent analysis using Focus (*22*).

RESULTS

Molecular Dynamics Simulations. Four simulations were run, each of which used the NMR structure of Pease and Wemmer (*11*) as a starting structure. The first simulation at 27 °C [apa(27 °C); 2 ns] was made to compare experimental (*14*) and simulated amide exchange protection factors as part of a study of the nature of fluctuations that underlie amide hydrogen exchange from peptide secondary structure (*20*, *21*). The low occurrence of backbone fluctuations in the C-terminal helix in the apa(27 °C) simulation prompted a longer simulation at higher temperature (67 °C) in which backbone fluctuations should be better represented [apa(67 °C); 2.4 ns]. It was observed in both the apa(27 °C) and the apa(67 °C) simulations that the Ala5 backbone NH made better hydrogen bond interactions with the Asn2 side chain amide than the Asn2 backbone carbonyl (the classical hydrogen bond acceptor in a β-turn; see below). This prompted the 27 and 67 °C simulations of the alanine substitution mutant [N2A(27 °C); 1 ns, and N2A(67 °C); 2 ns], as well as the experimental characterization of the apamin-N2A mutant described in the following sections. Description of the simulations is focused largely on the longer 67 °C simulations, although the general features described in the following section were also represented in the low-temperature simulations.

Figure 2 shows the starting and final structures of the high-temperature simulations [apa(67 °C) and N2A(67 °C)]. The starting structure of apamin is largely retained throughout the simulation [consistent with experimental observations that the structure of apamin is stable at least up to 80 °C (ref *12*; unpublished observations)]. The RMSD (backbone atoms) plateaus near 1.2 Å (27 °C) or drifts between around 2 and 1.3 Å (67 °C) (Figure 3). In the latter case, the drifts in RMSD are largely associated with the loss and reformation of helical conformations in the C-terminal residues Q16 and Q17 (not shown). The RMSD values in the apamin-N2A simulations reach higher values as compared to apamin in both low and high-temperature simulations (Figure 3), plateauing near 2 Å in the 27 °C simulation and 3 Å at 67 °C.

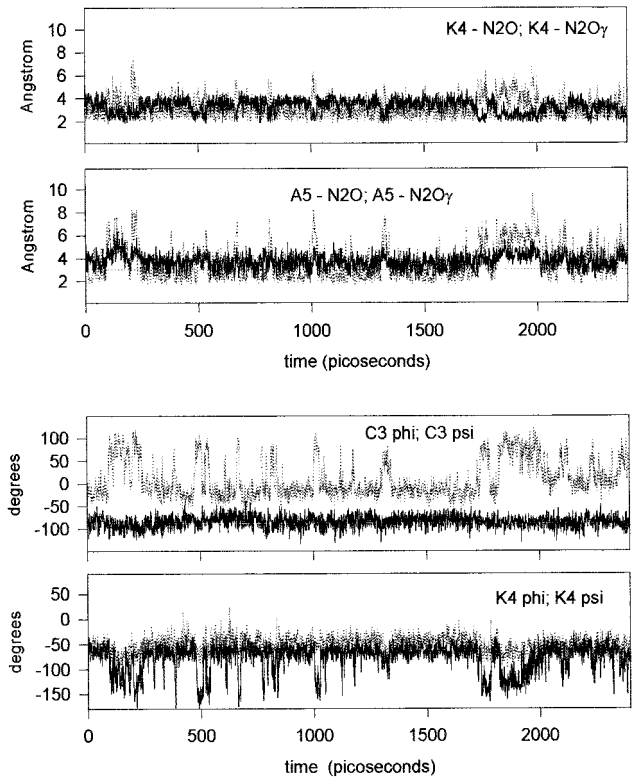

FIGURE 4: Characterization of β-turn parameters in apamin during molecular dynamics simulation in water at 67 °C. Top: evolution of NH to amide carbonyl distances for K4 and A5 amide NHs with carbonyl partners as indicated. Bottom: evolution of phi (bold traces) and psi (light traces) for the central pair of residues, C3 and K4, of the β-turn.

It is instructive to compare N-terminal β-turn stabilities in the two simulations in terms of potential hydrogen bond interactions, since this yields insight into the contribution of Asn2 to β-turn stability in apamin. Figures 4 and 5 illustrate the length of potential β-turn hydrogen bonds involving K4 and A5 backbone NHs. In the apa(67 °C) simulation, the overall β-turn geometry is retained throughout, despite some reversible fluctuations away from β-turn structure. The role of the Asn2 side chain as a hydrogen bond acceptor is particularly marked, with good hydrogen bond geometries involving both K4 and A5 NHs during much of the trajectory (Figure 4, top traces); in line with preliminary observations, hydrogen bonds involving Ala5 NH with the Asn2 side chain amide are more highly populated than those involving the Asn2 backbone carbonyl (Table 1). Despite the long separation between Ala5 NH and Asn2 backbone carbonyl, this distance remained constant (around 3.4 ± 0.5 Å) throughout the entire simulation consistent with the observed stability of the β-turn. The long separation between the potential β-turn hydrogen bond donor and acceptor observed in the simulations is also consistent with the chemical shift of Ala5 NH which is highly shielded, characteristic of a long hydrogen bond (*23*) (see Figure 9).

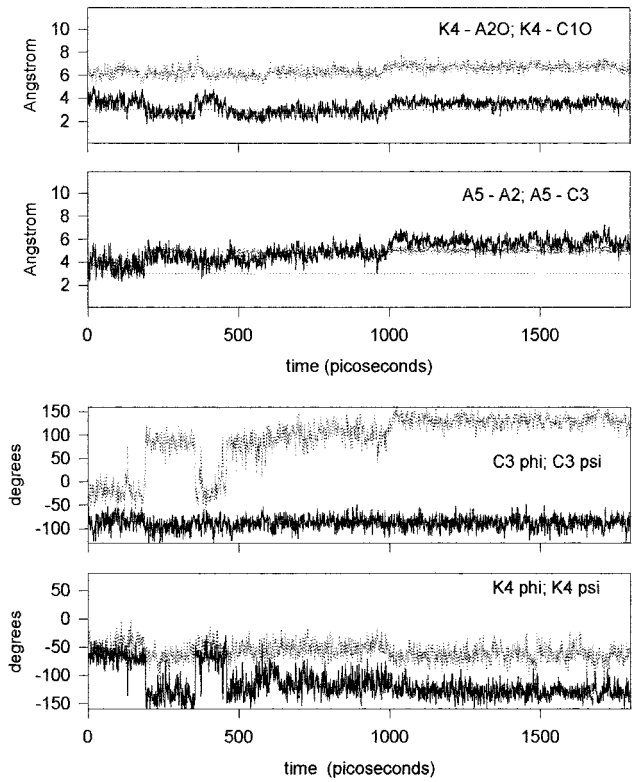

FIGURE 5: Characterization of β-turn parameters in apamin-N2A(par) during molecular dynamics simulation in water at 67 °C. Top: evolution of NH to amide carbonyl distances for K4 and A5 amide NH's with carbonyl partners as indicated. Bottom: evolution of phi (bold traces) and psi (light traces) for the central pair of residues, C3 and K4, of the β-turn.

Table 1: β-Turn Hydrogen Bonds during Apamin Simulation at 67 °C

amide	carbonyl partner	% H-bond[a]	% bifurcated[b]
Lys4	Asn2 backbone	31.3[c]	9.0
	Asn2 side chain	51.5	
Ala5	Asn2 backbone	13.8	4.5
	Asn2 side chain	40.8	
Lys4 + Ala5	Asn2 side chain		27.7

[a] Percentage of total trajectory in which H- -O distance $\leq$ 3.0 Å and N−H···O angle 180 ± 90°. [b] Percentage of trajectory in which hydrogen bond criteria (see footnote a) are satisfied for both hydrogen bonds simultaneously. [c] N−H···O angle is near 100° throughout.

The hydrogen bond properties of Lys4 and Ala5 backbone NHs in the N2A(67 °C) simulation are quite different. The separation between Ala5 NH and its β-turn carbonyl partner (Ala2 carbonyl) shifts in two steps from around 3.4 Å to 4.3 Å near 200 ps and 5.4 Å near 1 ns (Figure 5, top traces). This loss of the expected spatial relationship between β-turn residues i and i + 4 as the β-turn geometry is disrupted is associated with the rapid (near 200 ps) shift in the ϕ and ψ torsions of residues Cys3 and Lys4 away from canonical β-turn values (Figure 5, bottom trace). It is interesting that equivalent flips of the Cys3 and Lys4 ϕ and ψ torsions occur in the apa(67 °C) simulation (Figure 4, bottom traces). In the wild-type simulation, however, these flips are reversible, reverting within 20−100 ps to torsion values close to the starting values (Figure 4, bottom traces). Rapid, concerted flips of the central peptide unit of β-turns have been previously observed in simulations and were recently discussed in the context of protein crystal structures (ref *24* and references therein). The hydrogen bond interactions involving the Asn2 side chain are instrumental in maintaining the β-turn geometry during the wild-type simulation; as judged by an analysis of hydrogen bond geometries (H···O distance and N−H···O angle), these hydrogen bond interactions contribute significantly more to β-turn stability than those involving the backbone carbonyl of Asn2 (Table 1). A representative structure of hydrogen bonding within the β-turn is illustrated in Figure 6.

The N-terminal β-turn of apamin (residues Asn2−Ala5) is linked to the stable C-terminal helix directly via the Cys3−Cys 15 disulfide and less directly via the Cys1-Cys11 disulfide and the linking sequence of polypeptide (Figures 1 and 2). The stability of the C-terminal helical conformation is conveniently monitored in terms of the $NH_i \cdots OC_{i-4}$ distance that defines α-helical hydrogen bonds (Figures 7 and 8). At low pH, C11 NH is the first amide of the C-terminal helix whose exchange is stabilized by hydrogen bonding (*14*). The structure of the peptide in the linking sequence between the C-terminal helix and N-terminal segment (*11*) precludes an α-helical type hydrogen bond involving C11 NH (with the backbone carbonyl of Glu7), but this amide makes good hydrogen bond interaction with the Thr8 backbone carbonyl (3_{10} type) and Thr8 side chain hydroxyl oxygen; these interactions are also illustrated in Figures 7 and 8. Consistent with high C-terminal helical stability in apamin (see later sections) good alpha (or 3_{10}) helical hydrogen bonds are maintained throughout the entire apa(67 °C) simulation, with only minor fluctuations from helical geometries (Figure 7). In the N2A(67 °C) simulation, a transition near 500 ps irreversibly disrupts helical hydrogen bonds involving Cys11 and Ala12 NHs and results in fluctuations of α-helical hydrogen bonds involving Arg13 and Arg14 NHs (Figure 8).

The simulations indicate that stabilization of the N-terminal β-turn by hydrogen bond interactions involving the Asn2 side chain propagates to stabilize hydrogen bonded secondary structure throughout the polypeptide. The prediction that loss of these stabilizing hydrogen bonds in the mutant apamin-N2A will decrease conformational stability was tested experimentally as described in the following section.

Experimental Characterization of Apamin-N2A. Air Oxidation of Reduced Peptides. Oxidative formation of intramolecular disulfide bonds in wild-type apamin and apamin-N2A occurred with similar kinetics as determined by quantitation of reduced and oxidized species during the time course of oxidation (not shown). In each case, the oxidized peptides were less strongly retained on the reverse phase column than the parent reduced peptides. Oxidation of apamin-N2A resulted in two components produced in roughly equally proportions. Identification of characteristic NOEs between β-protons of disulfide-bonded cysteine residues (not shown) confirmed that these species are isomers having differently paired disulfides. The early eluting component has the wild-type cysteine pairing (Cys-1 with −11, and Cys-3 with −15, respectively). In this isomer, the N- and C-terminal sequences linked by the disulfides are parallel (Figure 1); this isomer is therefore designated apamin-N2A(par). The later eluting component has disulfides linking Cys-1 with −15, and Cys-3 with −11, respectively. In this isomer the extreme N-terminal and C-terminal sequences are antiparallel (Figure 1), and this

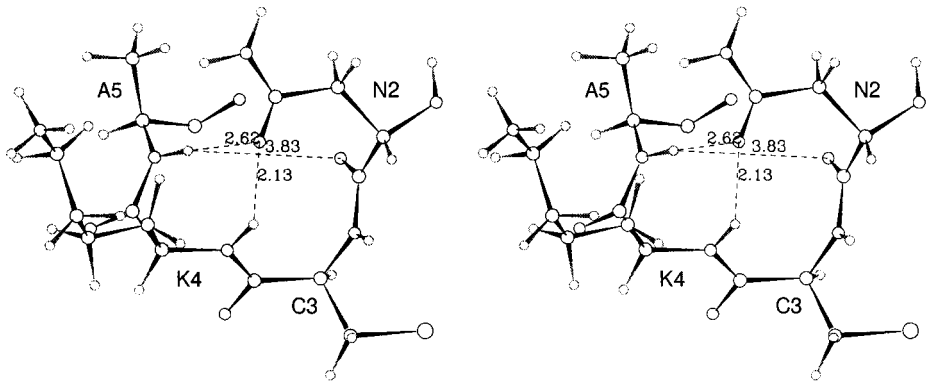

FIGURE 6: Representative hydrogen bonding within the Asn2-stabilized β-turn of apamin during molecular dynamics simulation in water at 67 °C. The structure is a snapshot taken at 1.580 ns of the 2.4 ns apa(67 °C) simulation.

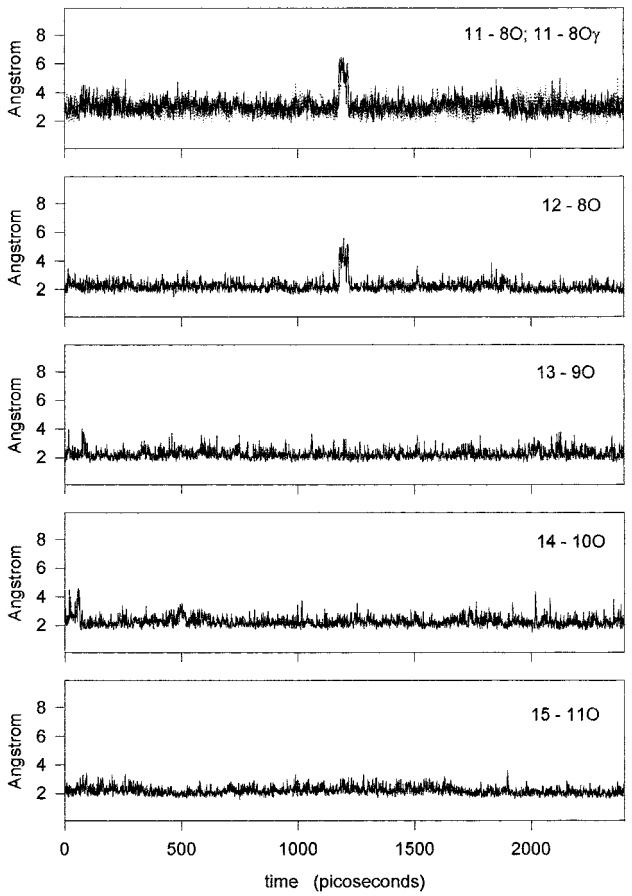

FIGURE 7: Characterization of helical hydrogen bonding for amide NHs in the apamin C-terminal helix during molecular dynamics simulation in water at 67 °C. The evolution of amide NH to carbonyl hydrogen bond distances is illustrated for α-helical (NH_i-CO_{i-4}) hydrogen bonds except for C11 NH (top panel) where hydrogen bond distances characteristic of an N-terminal helix capping motif are illustrated: C11 NH-T8 αCO (bold trace); C11 NH-T8 γCO (light trace).

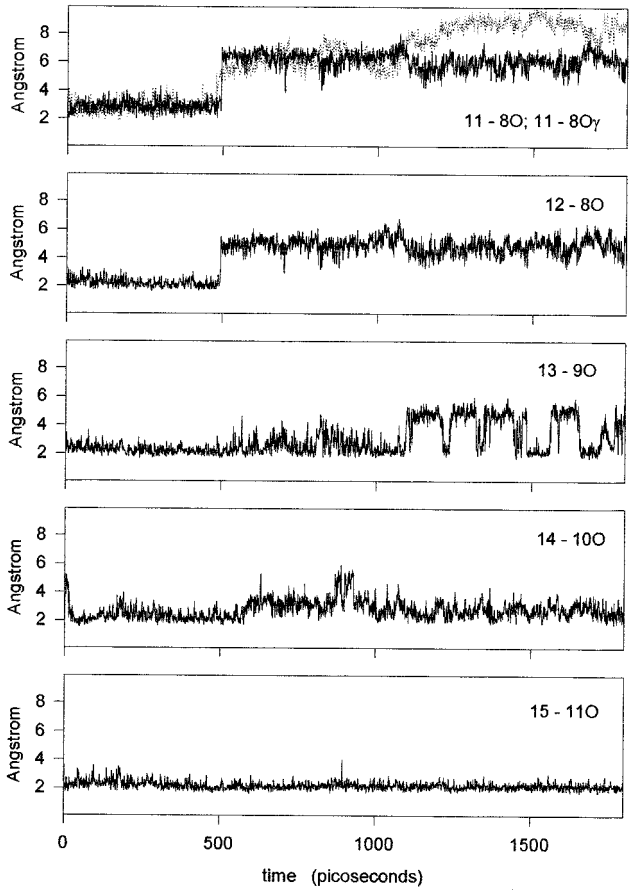

FIGURE 8: Characterization of helical hydrogen bonding for amide NHs in the apamin-N2A(par) C-terminal helix during molecular dynamics simulation in water at 67 °C. The evolution of hydrogen bond distances are illustrated as indicated in the legend to Figure 7.

isomer is designated apamin-N2A(anti). Each of the HPLC-purified peptides was shown to be fully oxidized and chemically homogeneous as observed by the loss of 4 mass units in the mass spectra, as compared with the fully reduced peptides.

Structures of Apamin, Apamin-N2A(par) and Apamin-N2A(anti). The NH and CHα chemical shifts of apamin and the N2A mutant with wild-type disulfide pairings [apamin-N2A(par)] are similar for the amino acids in the C-terminal helix but differ in the sequence C3-T8 (Figure 9). In each case, upfield shifts of CHα protons characteristic of helical conformations occur in the sequence A9 to Q17. The two peptides with wild-type disulfide pairings also show a periodicity in amide NH chemical shifts characteristic of curved or bent helices (*25*), with deshielded amide protons (characteristic of short hydrogen bonds) for A12 and C15 NHs on the helix face oriented toward the polypeptide "core", and longer hydrogen bonds on the helix face containing R13, R14, and Q16 NHs oriented toward the solvent. The amide NH,NH regions of the NOESY spectra of apamin, apamin-N2A(par), and apamin-N2A(anti) are

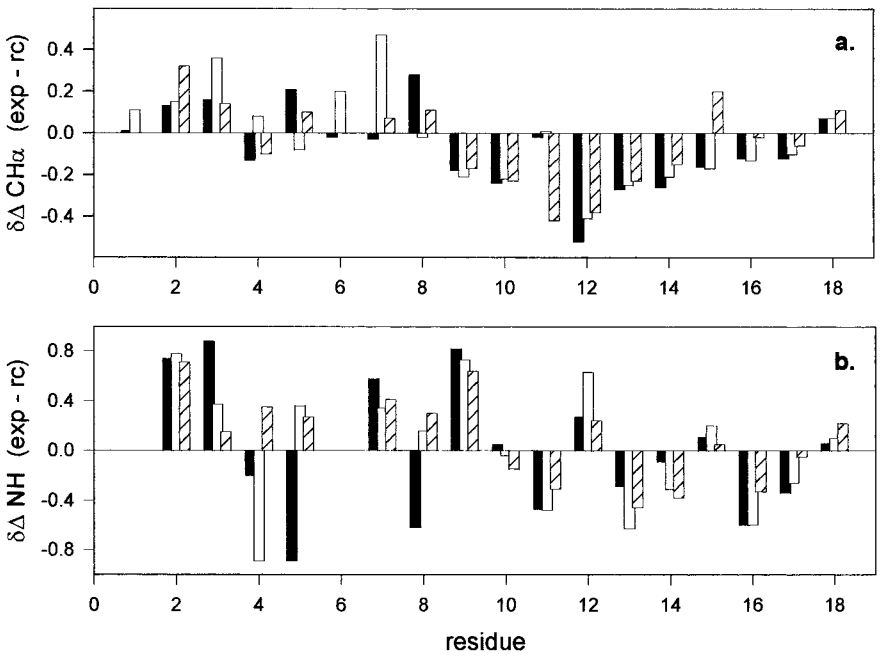

FIGURE 9: Deviation from random-coil chemical shifts (experimental − random coil) for (a) CHα and (b) backbone NH protons of apamin (black), apamin-N2A(par) (white), and apamin-N2A(anti) (hatch), in water at pH 3, 25 °C.

illustrated in Figure 10. Sequential NH,NH NOEs in the sequence encompassing residues A9 and Q16 demonstrate that the region of stable C-terminal helix in each peptide is equivalent. The location of stable helix is probably defined by intrinsic helical propensities in this sequence since nascent helical structure has been identified for these residues in fully reduced apamin (*26*), and the interactions involving C11 NH with the T8 backbone carbonyl (3_{10}-type helical hydrogen bond) and side chain hydroxyl (*11*) and identified in the MD simulations (Figure 7) are typical of an N-terminal helix capping motif (*27*).

The main structural changes in the N2A mutants occur in the N-terminal regions. In apamin, the N-terminal β-turn is partly defined by sequential NH,NH NOEs involving residues C3, K4, and A5 (refs *10* and *11*; Figure 10). These NOE interactions are lost in the N2A(anti) mutant (incorrect disulfide pairing). Weak sequential NH,NH NOE interactions involving the sequence N2, C3, and K4 in N2A(par) indicate that the turn required to accommodate the wild-type disulfide pairing now involves residues C1, A2, C3, and K4, although the low intensity of these NOEs (Figure 10, panel b), as compared to those of apamin (Figure 10, panel a) indicates that this turn is either less well-defined or is not fully populated in apamin-N2A(par). This shift in the location of the β-turn is consistent with the chemical shift of K4 NH which is highly shielded (like the amide NH of A5 in apamin) characteristic of the amide of the terminal residue of a turn (Figure 9; ref *8*). Otherwise, the set of NOEs identified in apamin-N2A(par) were very similar to those identified in apamin, and we were unable to identify NOEs that would define differences in the relation between the N-terminal turn residues and the C-terminal helix in apamin-N2A(par) as compared with the wild-type peptide.

Amide Exchange Protection Factors. pH-dependent exchange rate data were measured for wild-type apamin and the two disulfide isomers of apamin-N2A [i.e., apamin-N2A(par) and apamin-N2A(anti)]. Since exchange protection in the N2A mutants was low, relatively complete hydrogen−deuterium exchange data for these peptides were obtainable only at low pH* near pH^*_{min}. The exchange data at pH* 2.2 is measured near pH^*_{min} for the backbone amides of apamin (which has suppressed pH^*_{min} values due to the high overall net positive charge; ref *14*). Exchange rates at this pH have variable contributions from acid-catalyzed exchange and cannot be easily converted to exchange protection factors. The most suitable data for direct comparison of exchange protection factors is the pH* 3.2 data since base-catalyzed exchange contributions dominate at this pH in apamin (*14*). Also, the Glu7 side chain carboxylate is protonated at pH* 3.2 (ref *12* and references therein), and the additional contributions to conformational stability that result from hydrogen bonding and salt bridge interactions involving the Glu7 carboxylate (*14*) are absent at this pH [these effects are apparent in the enhanced exchange protection factor for apamin amides at pH* 4.2 (Table 2; see Discussion)].

Exchange protection factors for A5 NH (N-terminal turn) and A12, C13, R14, and C15 NHs (C-terminal helix) are highlighted in Table 2. Previous studies have shown that this set of amides defines the stable core of apamin; these amides respond together to factors that modulate the conformational stability of the peptide (*14*), as indicated in their enhanced protection factors at pH* 4.2 as the stable core of apamin is stabilized by interactions involving the Glu7 carboxylate (Table 2). It was previously suggested that exchange from these amides might result from a concerted breathing mode involving the helix and turn (*14*). Application of the Bai factors (*18*) that correct for sequence-dependent contributions to exchange (and were unavailable in 1986) demonstrates that exchange protection factor for amides in the C-terminal helix differ by a factor of up to 7-fold. For example, R13 NH has a low exchange protection factor as compared with other amides in the C-terminal helix, resulting probably from the location of this amide on the external helix face, as discussed above in the context of the amide chemical shifts

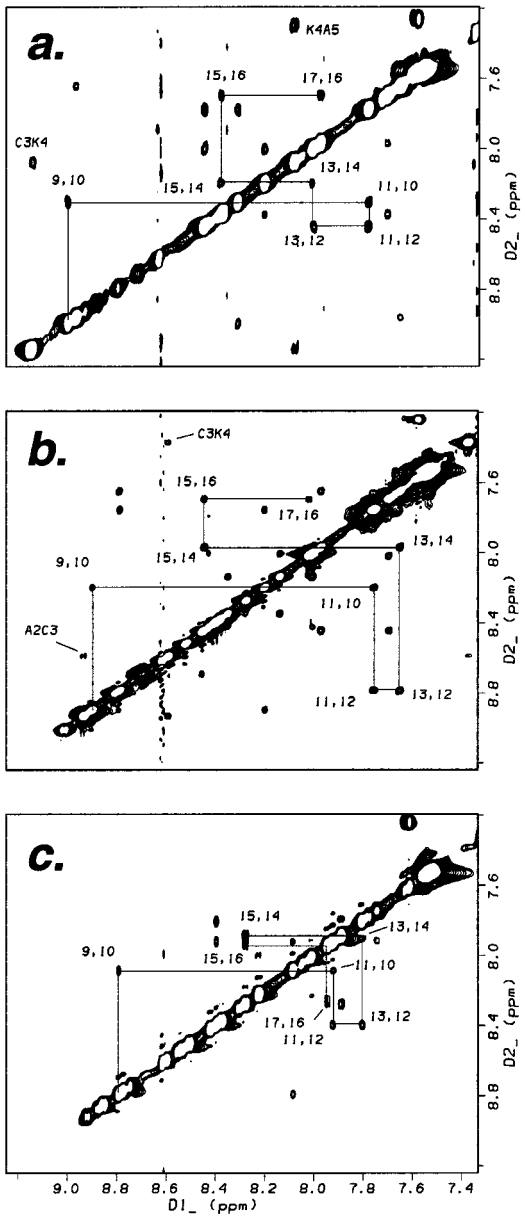

FIGURE 10: Amide NH,NH region of NOESY spectra of apamin (a), apamin-N2A(par) (b), and apamin-N2A(anti) (c) in water at pH 3, 25 °C. Sequential NH,NH NOEs that define the region of stable helix in the three peptides are linked in each spectra, and sequential amide NH,NH NOEs characteristic of a 4-residue (β)-turn are also indicated in the apamin and apamin-N2A(par) spectra.

in Figure 9; this amide might have an exchange mode that is independent from the other helical amides (residues 12, 14, and 15). On the other hand, it cannot be ruled out that differences in protection factors for residues within the helix results from variable accessibilities toward exchange in the transiently "open" state within such a concerted breathing mode. Despite differences in the absolute protection factor for amides within the C-terminal helix, the protection factors are reduced by similar amounts (9−11-fold) in apamin N2A as compared with the wild-type peptide. This reduction in conformational stability of the C-terminal helix provides an estimate of the contribution ($\delta\Delta G_{uf}$) of the Asn2 side chain to the stability of the β-turn of around 1.5 kcal M^{-1} at 20 °C. The larger decrease in exchange protection (~20-fold) of Ala5 NH in apamin-N2A, as compared with apamin, presumably results from the loss of the major hydrogen bond acceptor (Asn2 side chain amide carbonyl) for this amide as indicated in the simulations (Figure 5).

DISCUSSION

Dissection of Contributions to the Conformational Stability of Apamin. A common feature of polypeptide toxins that bind, and block ion channels with high affinity, is a high conformational stability that minimizes unfavorable entropic contributions to binding. In apamin, conformational stability is characterized by exchange protection of amides in the C-terminal helix [which contains the R13, R14 and Q17 residues that contribute most to receptor binding (*28*)] by up to 100-fold at pHs in which the Glu-7 side chain carboxyl is protonated (refs *13* and *14;* Table 2). This increases to around 1500-fold ($\delta\Delta G_{uf} \sim 4.5$ kcal M^{-1} at 300 K, where f and u denote, respectively, the folded, hydrogen-bonded state, and the transiently unfolded state from which exchange occurs), at pHs where the Glu-7 carboxylate forms a salt bridge with the N-terminal ammonium group (refs *12* and *14;* see below). The data in this, and previous studies, allow estimates of individual contributions to conformational stability of apamin in terms of amide exchange protection factors. The C-terminal helix is considerably stabilized in apamin-N2A(anti), with protection factors near 10 (Table 2), simply by linking to the N-terminal segment with two (non-wild-type) disulfide bonds. In general, the contribution of disulfide bonds depends on the size and conformation of the peptide loop(s) enclosed by the disulfides (*29*); in apamin-N2A(anti) these protection factors correspond to a stabilization free energy, $\delta\Delta G_{uf}$, of around 1.5 kcal M^{-1} at 20 °C.

Previous amide exchange measurements (*14*) indicated that the stability of the C-terminal helix in wild-type apamin is linked to that of the N-terminal β-turn, since A5 NH, hydrogen bonded within the β-turn, shares similar exchange protection as the amides of the C-terminal helix under a variety of conditions. The data presented here support the conclusion that the β-turn (N2, C3, K4, and A5) is a canonical Asn-stabilized motif (reviewed in ref *16*), since replacement of the Asn-2 residue with alanine, significantly destabilizes the β-turn. The loss of hydrogen-bonding interactions involving the Asn-2 side chain results in a near complete loss of exchange stability of A5 (and K4) backbone NHs (Table 2) but also destabilizes the C-terminal helix. The loss of exchange stability in the C-terminal helical amides in the sequence A12-C15 in apamin-N2A(par) of around 10−11-fold relative to wild-type apamin corresponds to a free energy (ΔG_{uf}) of around 1.5 kcal M^{-1} and is equivalent to the contribution of hydrogen bonding interactions involving the Asn2 side chain to the stability of the N-terminal β-turn. This value is similar to that obtained in the D46A mutation of the IgG binding domain of protein G [$\delta\Delta G = 1.7$ kcal M^{-1} (*30*)], where the D46 residue is residue i of an Asx-stabilized β-turn. The similarities in these values suggests that a value of 1.5−1.7 kcal M^{-1} is a good estimate of the context-independent contribution of an Asx_i residue to the stability of an Asx-stabilized β-turn.

A third contribution to conformational stability of apamin, explored in an earlier study (*14*), is the salt bridge and charge-stabilized hydrogen bonds identified by Okhanov et al. (*31*) that involve the Glu-7 carboxylate and N-terminal ammonium group. The effects of these electrostatic interactions

Table 2: Amide H−D Exchange Protection Factors for Apamin and Apamin-N2A Mutants[a]

	pH* 2.2			pH* 3.2			pH* 4.2	
res	apa	N2A(par)	N2A(anti)	apa	N2A(par)	N2A(anti)	apa	N2A(par)
C3	2.9	1.3	1.8	2.5	1.7	1.6	f[c]	f
K4	10.7	2.9	3.8	16.2	2.2	4.0	11.3	f
A5	9.5	1.1	nd[b]	**34.4**	**2.2**	**2.5**	134	f
T8	5.8	11.7	nd	5.6	9	nd	f	f
A9	1.6	2.1	2.4	0.4	0.4	0.8	f	f
L10	3.5	13.4	3.4	1.2	16	2.0	f	3.2
C11	24	13.8	nd	17	7.7	9.5	f	f
A12	65	26	9.0	**118**	**11.5**	**10.5**	**153**	2
R13	29	8.7	6.3	**37**	**6**	**5.7**	69	2.5
R14	46	19	7.1	**111**	**12**	**10.3**	184	13
C15	58	28	7.8	**289**	**26**	**11.0**	667	32
Q16	3.8	3.5	nd	30	7	9.0	36	f
Q17	1.0	1.1	nd	2.7	1.4	nd	15	

[a] 25 mM glycine, 25 mM sodium acetate buffer, 20 °C. [b] Not determined (due to resonance overlap in 1D spectrum). [c] Exchange rate to fast to measure by H/D exchange.

are observed in the increased exchange protection factors of the core amides of apamin (amides of A5 and A12-C15) on raising the pH* from 3.2 to 4.2 (Table 2). More detailed analysis (*14*) indicates that at low ionic strength, these interactions contribute around 1.6−1.8 kcal M^{-1} (ΔG_{uf}) to the thermodynamic stability of apamin in the pH range where the Glu-7 side chain and N-terminal amino group are charged. These three contributions (disulfide bonds, Asn-stabilized β-turn, and electrostatic interactions involving Glu-7 carboxylate and the N-terminal amino group), each close to 1.5 kcal M^{-1}, account for virtually the entire thermodynamic stability (ΔG_{uf}) of around 4.5 kcal M^{-1} at 20 °C measured from amide exchange protection factors (*14*). Other contributions to stability include the high intrinsic helical propensities of the C-terminal residues that give rise to nascent helix in the fully reduced peptide (*26*) and to high K_{ox} values for the disulfide Cys11, Cys15-pair (*32*).

Hydrogen Bonding within the Asn-2 Stabilized β-Turn in Apamin. The N-terminal β-turn in apamin is well-defined (*10*, *11*, *12*), with characteristic intraNH NOEs for backbone NHs in the sequence C3−K4−A5 (see Figure 10), characteristic NHCHα coupling constants, and slow amide exchange of Ala5 NH (see Table 2), which is expected to participate in a transannular hydrogen bond with the Asn2 backbone carbonyl. Slow exchange of K4 NH is proposed to result from hydrogen bonding with the Asn2 side chain amide (*11*, *12*), equivalent to a class 1 Asx-motif (Asx-β-turn) in the notation of the recent catalog of Asx-stabilized turns of Wan and Milner-White (*16*). Although conclusive conclusions cannot be drawn from simulations, those described here suggest that slow amide exchange of Ala5 NH does not result from a discrete hydrogen bond with the Asn2 backbone carbonyl (since the hydrogen bond distance fluctuates around 3.5 Å throughout the simulations) but is a consequence of the overall stability of the Asn-stabilized β-turn (Figure 6) that limits formation of exchange-competent interactions with water and/or hydroxyl ions. Amide exchange of Ala5 NH would then require fluctuations involving transient disruption of β-turn structure. The simulations indicate that these fluctuations (and those involving transient hydrogen bond disruption in the C-terminal helix) are not well-represented on the nanosecond time scale in apamin (Figures 4 and 7) but may be in apamin-N2A(par) (Figures 5 and 8).

Contribution of Asn-2 to Folding and Structure in Apamin. Pegoraro et al. (*32*) have proposed a folding pathway (Figure 6 of their paper) for apamin involving initial formation of a (non-wild-type) Cys11−Cys15 disulfide bond that "locks" the nascent helix, followed by disulfide exchange as the Cys3 thiolate displaces Cys11 by forming a (wild-type) disulfide with Cys15. The correct disulfide pairing relies on intrinsic stability of the N-terminal β-turn (*26*) which dictates the bicyclic wild-type disulfide pattern in which the N- and C-terminal peptide sequences are parallel (rather than antiparallel). Our study supports the importance of the stability of the N-terminal β-turn for correct folding, since the loss of stabilizing interactions involving the Asn2 side chain results in a fully oxidized peptide in which discrimination of disulfide pairings between parallel (Cys1, Cys11; Cys3, Cys15 wild-type) and antiparallel (Cys1, Cys15; Cys3, Cys11) arrangements is lost. The role of structure in the N-terminal sequence in directing disulfide pairings was demonstrated by Volkman and Wemmer (*33*) with a K4 deletion analogue of apamin that oxidized to the antiparallel pairing (see Figure 1).

In addition to promoting wild-type disulfide pairings and increasing the thermodynamic stability of the wild-type conformation, stabilizing interactions involving the Asn2 side chain have other effects on the wild-type structure. The A5-P6 peptide bond in apamin is largely in the trans conformation (no more than 10% of cis isomer; refs *10*, *11*, and *12*), whereas around 15% of the cis isomer exists in apamin N2A(par), and around 25% cis isomer exists in apamin-N2A(anti). Increased proportion of cis X−P peptide bonds have been found in other apamin analogues (*32*−*34*).

Conclusions. The Asn-stabilized β-turn in apamin provides a major contribution to the structural stability of the peptide and promotes the formation of wild-type disulfide pairings. The experimental characterization of the N2A mutant was undertaken following an analysis by dynamics simulations, demonstrating the value of simulations in guiding experimental approaches to polypeptide structure and dynamics. The results suggest that apamin may be a useful template for further characterizing amino acid-specific contributions to β-turn stability by exploiting the linkage of the C-terminal helix stability to that of the N-terminal β-turn.

ACKNOWLEDGMENT

We are grateful to Professor D. Wemmer for the coordinates of the apamin NMR structure and to Dr. Graham Bloomberg for excellent synthesis of the apamin peptides.

SUPPORTING INFORMATION AVAILABLE

Chemical shifts of the ^{1}H NMR spectra of apamin-N2A(par) and apamin-N2A(anti) in water (Table S-21). This material is available free of charge via the Internet at http://pubs.acs.org.

REFERENCES

1. Hutchinson, E. G., and Thornton, J. M. (1994) *Protein. Sci. 3*, 2207−2216.
2. Munoz, V., and Serrano, L. (1994) *Nature Struct. Biol. 1*, 399−409.
3. Rohl, C. A., Chakrabartty, A., and Baldwin, R. L. (1996) *Protein Sci. 5*, 2623−2637.
4. Smith, C. K., Withka, J. M., and Regan, L. (1994) *Biochemistry 33*, 5510−5517.
5. Munoz, V., Thompson, P. A., Hofrichter, J., and Eaton, W. A. (1997) *Nature 390* 196−199.
6. Kobayashi, N., Honda, S., Yoshii, H., and Munekata, E. (2000) *Biochemistry 39*, 6564−6571.
7. Niggemann, M., and Steipe, B. (2000) *J. Mol. Biol. 296*, 181−195.
8. Smith, J. A., and Pease, L. G. (1980) *CRC Crit. Rev. Biochem. 8*, 315−399.
9. Callewaert, G. L., Shipolini, R. A., and Vernon, C. A. (1968) *FEBS Lett. 1*, 111−113.
10. Wemmer, D. E., and Kallenbach, N. R. (1983) *Biochemistry 22*, 1901−1906.
11. Pease, J. H. B., and Wemmer, D. E. (1988) *Biochemistry 27*, 8491−8498.
12. Bystrov, V. F., Okhanov, V. V., Miroshnikov, A. I., and Ovchinnikov, Y. A. (1980) *FEBS Lett. 119*, 113−117.
13. Englander, S. W., and Kallenbach, N. R. (1983) *Quart. Rev. Biophys. 16*, 521−655.
14. Dempsey, C. E. (1986) *Biochemistry 25*, 3904−3911.
15. Tamaoki, H., Miura, R., Kusunoki, M., Kyogoku, Y., Kobayashi, Y., and Moroder, L. (1998) *Protein Eng. 11*, 649−659.
16. Wan, W.-Y., and Milner-White, E. J. (1999) *J. Mol. Biol. 286*, 1633−1649.
17. Wuthrich, K. (1986) *NMR of Proteins and Nucleic Acids*, J. Wiley, N. Y., N. Y.
18. Bai, Y., Milne, J. S., Mayne, L., and Englander, S. W. (1993) *Proteins: Struct. Funct. Genet. 17*, 75−86.
19. Kim, P. S., and Baldwin, R. L. (1982) *Biochemistry 21*, 1−6.
20. Gibbs, N., Sessions, R. B., Williams, P. B., and Dempsey, C. E. (1997) *Biophys. J. 72*, 2490−2495.
21. Sessions, R. B., Gibbs, N., and Dempsey, C. E. (1998) *Biophys. J. 74*, 138−154.
22. Osguthorpe, D. J., and Dauber-Osguthorpe, P. (1992) *J. Mol. Graphics 10*, 178−184.
23. Wagner, G., Pardi, A., and Wuthrich, K. (1983) *J. Am. Chem. Soc. 105*, 5948−5949.
24. Gunasekaran, K., Gomathi, L., Ramakrishnan, C., Chandrasekhar, J., and Balaram, P. (1998) *J. Mol. Biol. 284*, 1505−1516.
25. Kuntz, I. D., Kosen, P. A., and Craig, E. C. (1991) *J. Am. Chem. Soc. 113*, 1406−1408.
26. Xu, X., and Nelson, J. W. (1994) *Biochemistry 33*, 5253−5261.
27. Aurora, R., and Rose, G. D. (1998) *Protein Sci. 7*, 211−38.
28. Labbejullie, C., Granier, C., Albericio, F., Defendini, M. L., Ceard, B., Rochat, H., and VanRietschoten, J. (1991) *Eur. J. Biochem. 196*, 639−645.
29. Creighton, T. E. (1994) *Proteins: Structures and Molecular Properties*, W. H. Freeman, New York.
30. McCallister, E. L., Alm, E., and Baker, D. (2000) *Nature Struct. Biol. 7*, 669−673.
31. Okhanov, V. V., Afanaseev, V. A., Gurevich, A. Z., Elyakov, E. G., Miroshnikov, A. I., Bystrov, V. F., and Ovchinnikov, Yu. A. (1980) *Sov. J. Bioorg. Chem. (Engl. Transl.) 6*, 840−864.
32. Pegoraro, S., Fiori, S., Cramer, J., Rudolph-Bohner, S., and Moroder, L. (1999) *Protein Sci. 8*, 1605−1613.
33. Volkman, B. F., and Wemmer, D. E. (1997) *Biopolymers 41*, 451−460.
34. Fiori, S., Pegoraro, S., Rudolph-Bohner, S., Cramer, J., and Moroder, L. (2000) *Biopolymers 53*, 550−564.

BI002044Q